Sensors and Materials, Vol. 36, No. 3 (2024) 1105–1113
MYU Tokyo

S & M 3584

Substrate-integrated Waveguide Bandpass Filter for 5G Applications

Jian-Mei Huang, Hai-Tao Xing, and Zhong-Hua Ma*

School of Marine Information Engineering, Jimei University,
No.183, Yinjiang Road, Jimei District, Xiamen, Fujian 361021, China

(Received June 26, 2023; accepted March 8, 2024)

Keywords: substrate-integrated waveguide (SIW), bandpass filter, 5G, millimeter wave (mm-wave)

In this work, a millimeter wave (mm-wave) bandpass filter consisting of six resonant cavities for 5G communication is designed on the basis of a substrate-integrated waveguide (SIW). The bandpass characteristics of the SIW filter are achieved through magnetic coupling, which is accomplished by adjusting the size of the openings between neighboring resonant cavities. The measured fractional bandwidth is 3.56% (24.8–25.7 GHz), with an insertion loss of 0.88 dB at the center frequency of 25.25 GHz, and the in-band return loss is better than 12 dB. The simulated results of this filter show excellent agreement with the measured results. It exhibits low loss, simple structure, low cost, ease of integration with other electromagnetic systems, including sensor systems, and suitability for use in 5G mm-wave bands.

1. Introduction

With the high-speed, large-capacity, and low-latency data transmission requirements of 5G communication, the millimeter wave (mm-wave) communication spectrum has attracted considerable attention.(1) As a key component to ensure the communication quality of the whole mm-wave communication system, the design of a mm-wave filter has become a hot research topic.(2)

The substrate-integrated waveguide (SIW) is a new waveguide structure that combines the advantages of both waveguides and microstrip lines. For example, it possesses advantages such as high quality factor, large power capacity, low cost, low radiation loss, and easy integration with planar circuits. The introduction of the SIW structure in mm-wave filter design is a practical and feasible method, which is conducive to optimizing the filter size and obtaining excellent filtering performance.

In recent years, various structures of SIW filters have been proposed successively. Augustine and Vinoy from the Indian Academy of Sciences designed a SIW filter with 11 cavities arranged in a zigzag pattern, operating frequency ranges from 25.25 to 29.5 GHz with a fractional bandwidth of 19.5%, and an average insertion loss of 4.73 dB in the passband.(3) Good out-of-band suppression is achieved through the cross-coupling of the cavities. However, the design is

*Corresponding author: e-mail: mzhxm@jmu.edu.cn
https://doi.org/10.18494/SAM4561

ISSN 0914-4935
https://myukk.org/

complex and the insertion and return losses are large. Professor Yang's team at the State Key Laboratory of Millimeter Waves, Southeast University, added machine learning into the optimization of SIW filter models and proposed two wideband SIW bandpass filters for the 5G mm-wave band with an insertion loss less than 1.5 dB, an out-of-band rejection of 35 dB, and 3 dB bandwidths of 13.09 and 22.11%.[4]

Chen and Wu designed dual-band fourth-order cross-coupled bandpass filters using a negative coupling structure, including both passive load-coupled and active load-coupled configurations.[5] The two novel SIW filters have center frequencies of 20.5 GHz and passband widths of 700 and 800 MHz. They exhibit excellent selectivity, with insertion losses of 0.9 and 1.0 dB in the passbands.

Zheng *et al.* presented the Ka-band multilayer SIW bandpass filter with a vertically laminated three-dimensional structure and fabricated by the low-temperature co-fired ceramic (LTCC) technique.[6] The coupling between adjacent aperture cavities is achieved by a narrow slot between different layers. This SIW bandpass filter has a center frequency of 27.73 GHz, an insertion loss of 1.74 dB, and a 3 dB bandwidth ranging from 26.30 to 29.08 GHz.

Zhou *et al.* proposed adjustable passbands based on an assembled multimode resonant printed circuit board for SIW bandpass filters using one layer, two layers, and three layers of PCB to tune the single-band, dual-band, and triple-band responses, respectively. The in-band return loss in the K-band is better than 22.1 dB and the minimum in-band insertion loss is 0.5 dB.[7]

As an important part of RF sensor systems, SIW-based filters have been applied to many fields. The SIW bandpass filters mentioned above have the advantages of wide passband and good out-of-band rejection performance, but they generally suffer from a higher insertion loss. The SIW filter proposed by Zhou *et al.* above achieves an insertion loss as low as 0.5 dB, but it requires a multilayer structure, which makes integration into systems more challenging.

In this study, we design the bandpass filter operating in mm-wave with the SIW structure, which achieves the bandpass characteristics by adjusting the size of the coupling openings between adjacent cavities. Compared with other similar SIW bandpass filters, the filter proposed in this paper exhibits excellent insertion and return losses, demonstrating good competitiveness. In Sect. 2, we describe the fundamental principles of SIW. In Sect. 3, we describe in detail the SIW filter's design and simulation process. To verify the scheme proposed in this paper, the device was fabricated on a Rogers 5880 substrate. The measurement results described in Sect. 4 are in good agreement with the simulation results. Finally, we provide the conclusions in Sect. 5.

2. Fundamental Principles of SIW

SIW was initially proposed by the Canadian scholar Professor K. Wu. It consists of a dielectric substrate, upper and lower metal layers, and two sets of metal via holes.[8] The two sets of metal via holes form magnetic walls, connecting the upper and lower metal surfaces of the substrate to create an electric wall. The basic structure of SIW is shown in Fig. 1, where the width of the short side is W_{SIW}, the width of the long edge is L_{SIW}, the via hole diameter is d, the via hole spacing (center-to-center distance) is s, and the thickness of the dielectric substrate is h.

Owing to the presence of gaps between the metalized via holes, there are certain requirements

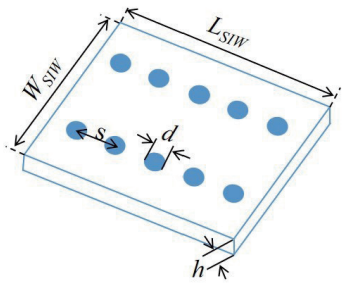

Fig. 1. (Color online) Diagram of SIW structure.

for the gap size in the actual design in order to prevent electromagnetic wave leakage. If the via hole diameter d and the adjacent via hole spacing s satisfy Eq. (1), electromagnetic leakage can generally be neglected.(9)

$$\begin{cases} d < 0.2\lambda_g \\ d < 0.2W_{SIW} \\ s < 2d \end{cases} \tag{1}$$

According to Eq. (1), as s/d decreases, it becomes more challenging for electromagnetic waves to leak between the apertures. However, from a practical perspective, excessively small hole diameters and aperture spacings undoubtedly pose difficulties in actual production. Therefore, for SIW structures, it is crucial to select appropriate values for d and s, ensuring minimal leakage loss and ease of fabrication for the entire structure.

The fundamental mode of SIW is the TE_{101} mode, which corresponds to the TE_{m0n} mode, where m and n represent the mode numbers along the x- and z- directions, respectively. The resonant frequency of the SIW resonance cavity is given by(10)

$$f_{TE_{m0n}} = \frac{c}{2\sqrt{\mu_r \varepsilon_r}} \sqrt{\left(\frac{m}{W_{eff}}\right)^2 + \left(\frac{n}{L_{eff}}\right)^2} . \tag{2}$$

Here, c is the speed of light equal to 3×10^{11} mm/s, μ_r is the relative permeability, ε_r is the dielectric constant, and W_{eff} and L_{eff} are the equivalent width and equivalent length of SIW, respectively. Taking into account the effect of via holes, the calculation formulas of W_{eff} and L_{eff} are modified as follows.(11)

$$\begin{cases} W_{eff} = W_{SIW} - \dfrac{d^2}{0.95s} + \dfrac{0.1d^2}{W_{SIW}} \\ L_{eff} = L_{SIW} - \dfrac{d^2}{0.95s} + \dfrac{0.1d^2}{L_{SIW}} \end{cases} \tag{3}$$

The dimensional parameters of the filter are preliminarily determined from Eqs. (2) and (3).

With these parameters, the model of the SIW fourth-order coupled bandpass filter is established in the High-Frequency Structure Simulator (HFSS) software, as shown in Fig. 2.

3. Design and Simulation

Figure 2 shows the structure of the proposed SIW mm-wave bandpass filter. The adopted substrate here is Rogers 5880 with a relative permittivity of 2.2, a loss tangent of 0.0009, and a dielectric thickness of 31 mil. The input and output ports are structured with a microstrip line direct transition conversion structure. There is an opening in the middle of the metal via-hole wall between adjacent resonant cavities to realize coupling. The coupling strength is closely related to the length of the coupling openings between adjacent resonant cavities. By systematically modifying the structural parameters of SIW and observing the impact of these parameters on the performance of the filter, the optimal structural parameters listed in Table 1 were finally obtained.

The coupling mechanism among the resonators of the proposed filter is shown in Fig. 3. S represents the source excitation, L represents the load, and R_1 to R_6 represent six SIW resonant cavities. R_1^3 represents the TE_{103} mode in the rectangular resonant cavity, whereas R_2^1–R_6^1

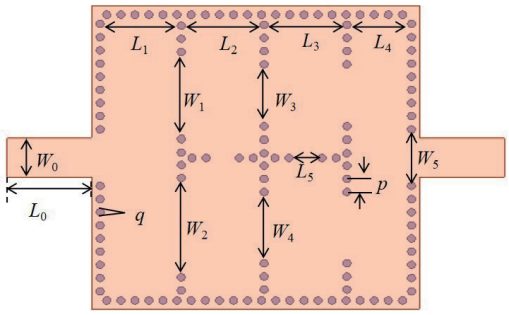

Fig. 2. (Color online) Structure of proposed SIW bandpass filter.

Table 1
Optimal parameters of proposed filter (unit: mm).

W_0	W_1	W_2	W_3	W_4	W_5	p
2.5	5.6	5.8	4	4.2	3.6	0.85
L_0	L_1	L_2	L_3	L_4	L_5	q
5.1	4.9	5	5	3.9	2	0.48

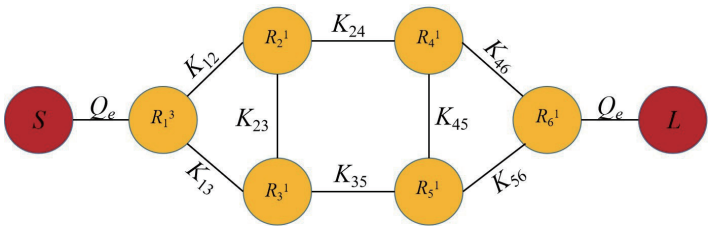

Fig. 3. (Color online) Coupling topology of proposed filter.

correspond to the TE_{101} mode in the resonant cavity. Q_e is the external quality factor, and K_{ij} represents the coupling coefficient between the i-th and j-th resonant cavities ($i, j = 1, 2, 3, 4, 5, 6$ and $i \neq j$). According to the theory of coupled resonators, the external quality factor and the coupling coefficients between adjacent resonant cavities can be determined using the following formulas:[12]

$$Q_e = \frac{f_0}{\Delta f_{\pm 90^\circ}}, \tag{4}$$

$$K_{ij} = \frac{f_j^{\,2} - f_i^2}{f_j^2 + f_i^2}. \tag{5}$$

Here, f_0 is the resonant frequency of the first resonant cavity excitation port and $\Delta f_{\pm 90^\circ}$ is determined from the frequency at which the phase shifts ±90° relative to the absolute phase at f_0. The lower resonant frequency point f_i and the higher frequency point f_j are obtained by HFSS eigenmode simulation.

The filter utilizes coupling opening for magnetic coupling and the electric field distribution diagram provides a visual representation of the coupling effect between resonant cavities. The electric field distribution of the SIW bandpass filter is given in Fig. 4. Figure 5 shows the frequency response curve of the SIW bandpass filter obtained from the simulation. The filter operating frequency ranges from 24.845 to 25.693 GHz, with a 3 dB passband width of 848 MHz and a fractional bandwidth of 3.36%. The insertion loss at the center frequency of 25.269 GHz is 0.79 dB and the reflection coefficient within the passband is less than −12 dB. The filter is suitable for applications in the 5G-FR2 mm-wave band.

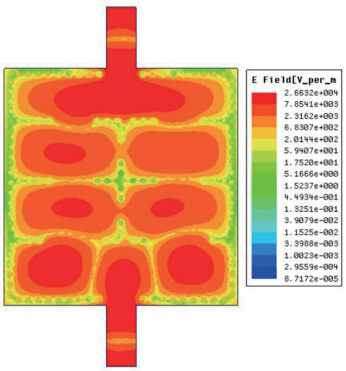

Fig. 4. (Color online) Electric field distribution of SIW bandpass filter.

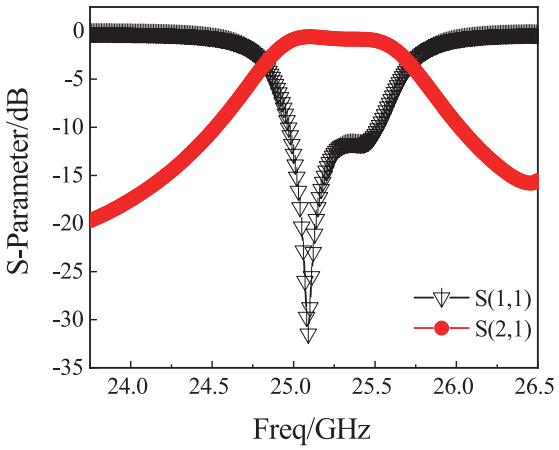

Fig. 5. (Color online) Simulation S-parameter curves of filter.

4. Measurement Results and Comparison

To validate the proposed SIW bandpass filter, the filter is fabricated on the Rogers 5880 substrate and a photograph is shown in Fig. 6. The area of this filter is 30 × 19.5 mm² and the thickness is 31 mil. Figure 7 illustrates the testing setup for the SIW bandpass filter. A Ceyear vector network analyzer model 3672D was employed to measure its characteristic curves. The filter's input and output ports were connected to the vector network analyzer's two ports via SMA connectors and RF cables.

The frequency response curves of the measured SIW bandpass filter are shown in Fig. 8. The insertion loss is 0.88 dB at the center frequency of 25.25 GHz. The 3 dB fractional bandwidth of the bandpass filter is 3.56% from 24.8 to 25.7 GHz, and the reflection coefficients in the passband are less than −12 dB. Compared with the simulation results, the actual measured SIW bandpass filter has superior transmission coefficient and bandwidth. Additionally, some discrepancies between the simulated and measured curves can be attributed to manufacturing and measurement errors. In general, both simulations and measurements show good agreement.

Table 2 shows the comparison between the proposed SIW mm-wave bandpass filter and some other reported filters. Augustine and Vinoy proposed the SIW bandpass filter that exhibits good out-of-band rejection and a wide bandwidth,[3] but it has a large in-band insertion loss of

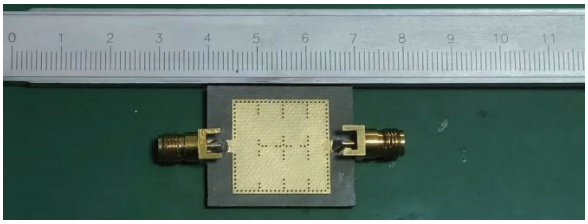

Fig. 6. (Color online) Physical depiction of designed bandpass filter.

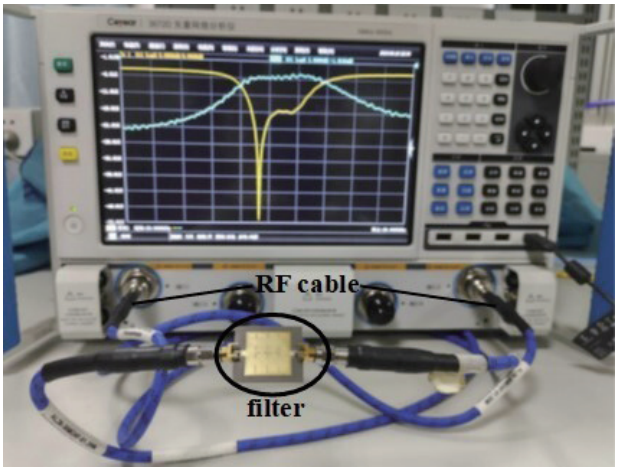

Fig. 7. (Color online) Diagram of measurement setup.

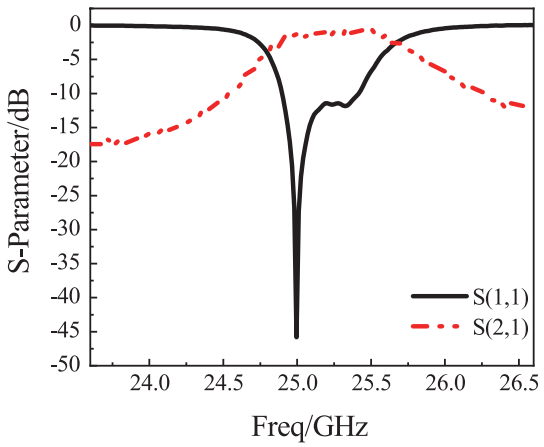

Fig. 8. (Color online) Measured S-parameter curves of filter.

Table 2
Comparison with other works.

Ref.	Frequency Range (GHz)	ε_r	Return loss (dB)	Insertion loss (dB)	Size (λ_0^3)	Layer
3	24.25–29.5	3.66	>10	4.73	$3.49\lambda_0 \times 1.33\lambda_0 \times 0.05\lambda_0$	1
6	26.30–29.08	6.2	>10	1.74	$0.63\lambda_0 \times 0.38\lambda_0 \times 0.12\lambda_0$	4
13	131.3–149.6	5.9	>11	1.913	$2.14\lambda_0 \times 0.37\lambda_0 \times 0.09\lambda_0$	1
14	13.3–13.9	3.55	>15	<2.5	$3.2\lambda_0 \times 0.59\lambda_0 \times 0.014\lambda_0$	1
15	8.24–8.76	3.66	>10	1.79	$1.1\lambda_0 \times 1.05\lambda_0 \times 0.001\lambda_0$	4
16	19.7–20.3	2.2	>20	>1.7	$1.88\lambda_0 \times 1.42\lambda_0 \times 0.034\lambda_0$	1
This work	24.8–25.7	2.2	>12	0.88	$2.5\lambda_0 \times 1.625\lambda_0 \times 0.07\lambda_0$	1

4.73 dB. In Ref. 6, a four-layer SIW bandpass filter in the Ka band was fabricated using LTCC technology. This filter had a low insertion loss, but the four-layer structure made integration more challenging. Wong *et al.* presented a mm-wave SIW filter with four nonuniform slots.[13] This filter exhibits an insertion loss of 1.913 dB at the center frequency, which shows a significant insertion loss. In Ref. 14, the direct transition structures were used at both ends of the SIW bandpass filter. However, the filter has slightly large dimensions and a high insertion loss. Shen and Zhu proposed a compact SIW filter with three vertically stacked cavities.[15] The filter has a compact size, and two transmission zeros can be independently controlled. However, the structure is complex and not easily integrated. As shown in Ref. 16, two K-band cross-coupled SIW filters were designed at the same center frequency with the same bandwidth. The measured return loss was better than 20 and 15 dB, and the minimum insertion loss was approximately 1.7 and 1.8 dB. These two filters had good reflection coefficients, but narrow bandwidths and high insertion losses. Comparatively, the proposed design demonstrates a simple structure, an easy integration with other electronic devices, a low insertion loss, and reflection coefficients superior to those of the referenced filters. Thus, it holds significant potential for applications in the 5G era.

5. Conclusions

A single-layer fourth-order SIW bandpass filter based on the PCB process is proposed in this paper, which is simple in structure and easy to integrate with other electronic devices. The measured 3 dB bandwidth range of the SIW bandpass filter is 24.8–25.7 GHz, with a high quality factor. The insertion loss at the center frequency of 25.25 GHz is measured to be 0.88 dB and the in-band return loss is better than 12 dB. Simulation and measurement results are almost consistent. In RF sensors, bandpass filters are commonly used to fulfill system signal processing requirements. The proposed filter holds great potential in various fields, especially in 5G mm-wave band applications. Certainly, the proposed SIW filter's footprint can be further reduced. In the future, the miniaturization of the filter can be achieved through the optimization of cavity dimensions and feeding structures.

Acknowledgments

This work was supported by the Fujian Natural Science Foundation Project (2022J01823) and Leading project of Fujian Science and Technology Plan (2023H0015).

References

1 T. S. Rappaport, S. Sun, R. Mayzus, H. Zhao, Y. Azar, K. Wang, G. N. Wong, J. K. Schulz, M. Samimi, and F. Gutierrez: IEEE Access **1** (2013) 335. https://doi.org/10.1109/ACCESS.2013.2260813
2 W. Hong, Z. H. Jiang, C. Yu, D. Hou, H. Wang, C. Guo, Y. Hu, L. Kuai, Y. Yu, Z. Jiang, Z. Chen, J. Chen, Z. Yu, J. Zhai, N. Zhang, L. Tian, F. Wu, G. Yang, Z.-C. Hao, and J. Y. Zhou: IEEE J. Microwaves **1** (2021) 101. https://doi.org/10.1109/JMW.2020.3035541
3 A. Augustine and K. J. Vinoy: Proc. 2022 IEEE Microwaves, Antennas, and Propagation Conf. (IEEE, 2022) 1283. https://doi.org/10.1109/MAPCON56011.2022.10047406
4 Y. Yang, Q. Wu, H. Wang, and W. Hong: Proc. 2021 13th Int Symp. Antennas, Propagation and EM Theory (IEEE, 2021) 1. https://doi.org/10.1109/ISAPE54070.2021.9753160
5 X.-P. Chen and K. Wu: IEEE Trans. Microwave Theory Technol. **56** (2008) 142. https://doi.org/10.1155/2018/9737219
6 P. Zheng, Z. Liu, M. Ma, Y. Wang, F. Liu, and Y. Li: Wireless Commun. Mobile Comput. **2018** (2018) 1. https://doi.org/10.1155/2018/9737219
7 X. Zhou, G. Zhang, J. Zheng, W. Tang, and J. Yang: IEEE Trans. Circuits Syst. II Express Briefs **69** (2022) 3386. https://doi.org/10.1109/TCSII.2022.3157713
8 K. Wu, D. Deslandes, and Y. Cassivi: Proc. 6th Int. Conf. Telecommunications in Modern Satellite, Cable and Broadcasting Service (IEEE, 2003) P-III. https://doi.org/10.1109/TELSKS.2003.1246173
9 D. Deslandes and K. Wu: IEEE Trans. Microwave Theory Technol. **54** (2006) 2516. https://doi.org/10.1109/TMTT.2006.875807
10 Y. Cassivi, L. Perregrini, P. Arcioni, M. Bressan, K. Wu, and G. Conciauro: IEEE Wireless Commun. Lett. **12** (2002) 333. https://doi.org/10.1109/LMWC.2002.803188
11 F. X and K. W: IEEE Trans. Microwave Theory Technol. **53** (2005) 66. https://doi.org/10.1109/TMTT.2004.839303
12 J.-S. Hong: Microstrip Filter for RF/Microwave Applications (John Wiley & Sons, 2011) 2nd ed., Chap. 3. https://doi.org/10.1002/0471221619
13 S. W. Wong, K. Wang, Z.-N. Chen and Q.-X. Chu: IEEE Trans. Compon. Packag. Manuf. Technol. **4** (2014) 316. https://doi.org/10.1109/TCPMT.2013.2285388
14 O. I. Hussein, K. A. A. Shamaileh, Dib, N. I. Dib, A. Nosrati, S. Abushamleh, D. G. Georgiev, Devabhaktuni, and V. K. Devabhaktuni: IEEE Access **8** (2020) 139706. https://doi.org/10.1109/ACCESS.2020.3012994

15 W. Shen and H.-R. Zhu: IEEE Microwave Wireless Compon. Lett. **30** (2020) 327. https://doi.org/10.1109/LMWC.2020.2969560
16 F. Zhu, W. Hong, J. X. Chen, and K. Wu: IEEE Microwave Wireless Compon. Lett. **22** (2012) 366. https://doi.org/10.1109/LMWC.2012.2228174

About the Authors

Jian-Mei Huang was born in 2002 in Fujian Province, China. She is currently pursuing her B.S. degree with the Department of Communication Engineering at Jimei University, Fujian Province, China. Her research interests are in mm-wave and antenna technologies. (hjm@jmu.edu.cn)

Hai-Tao Xing was born in 1983 in Shandong, China. In 2010, he obtained a master's degree in communication and information engineering from Ningbo University. At present, his main research interests are in embedded systems, artificial intelligence, and IoT. (xht2005@jmu.edu.cn)

Zhong-Hua Ma was born in Gansu, China, in 1973. He received his Ph.D. degree in microelectronics from Lanzhou University in 2018. His present research interests include antenna techniques, RF circuit design, RFID systems, and IoT. (mzhxm@jmu.edu.cn)